

This is an Open Access document downloaded from ORCA, Cardiff University's institutional repository: <https://orca.cardiff.ac.uk/id/eprint/161311/>

This is the author's version of a work that was submitted to / accepted for publication.

Citation for final published version:

Li, Xin, Rui, Peng, Ye, Tongqi, Yao, Xin, Zhou, Rulong, Li, Dongdong, Wang, Sheng, Carter, James H. and Hutchings, Graham J. 2023. Hydrogenolysis of 5-hydroxymethylfurfural by in situ produced hydrogen from water on an iron catalyst. *Catalysis Science & Technology* 13 (11) , pp. 3366-3374. 10.1039/D3CY00027C

Publishers page: <http://dx.doi.org/10.1039/D3CY00027C>

Please note:

Changes made as a result of publishing processes such as copy-editing, formatting and page numbers may not be reflected in this version. For the definitive version of this publication, please refer to the published source. You are advised to consult the publisher's version if you wish to cite this paper.

This version is being made available in accordance with publisher policies. See <http://orca.cf.ac.uk/policies.html> for usage policies. Copyright and moral rights for publications made available in ORCA are retained by the copyright holders.



# Hydrogenolysis of 5-hydroxymethylfurfural by in situ produced hydrogen from water on an iron catalyst†

Xin Li,<sup>‡a</sup> Peng Rui,<sup>‡a</sup> Tongqi Ye,<sup>id \*a</sup> Xin Yao,<sup>a</sup> Rulong Zhou,<sup>id b</sup> Dongdong Li,<sup>b</sup> Sheng Wang,<sup>c</sup> James H. Carter<sup>id \*d</sup> and Graham J. Hutchings<sup>id d</sup>

The hydrogenolysis of 5-hydroxymethylfurfural in a flow reactor was investigated over iron catalysts in the presence of water. The reaction proceeds in the presence of hydrogen or an inert atmosphere. Isotopic substitution studies where deuterium was used instead of water proved that the hydrogen in the final product can originate from water. The role of water was further investigated and it was found that it can re-oxidise the catalyst during the reaction. X-ray diffraction was used to identify the active phases present during and after the reaction. Density functional theory calculations revealed that the adsorption of the substrate is rather strong on Fe(110), and this may explain the formation of humins during the reaction, which is regarded as the main limitation of the current catalyst.

## 1. Introduction

The world demand for alternative sources of energy and chemicals stimulates the research needed to produce chemicals from renewable biomass resources. As one of the ten bio-based platform chemicals, 5-hydroxymethylfurfural (HMF) is gaining significance in the context of sustainable economies.<sup>1</sup> It can be produced by the dehydration of glucose or fructose or by one-pot hydrolysis/dehydration of cellulose with the presence of catalysts.<sup>2</sup> HMF can be used to produce 5-methylfuraldehyde (5-MF), 2,5-bis(hydroxymethyl)furan (BHMF) and dimethylfuran (DMF) by hydrogenation/ hydrogenolysis process (Scheme 1), or to produce 2,5-diformylfuran (DFF) and dicarboxylic acid (FDCA) by dehydrogenation/oxidation process.<sup>3</sup>

In recent years, increasing attention has been devoted to the transformation of HMF to 5-MF, which is considered as an important chemical intermediate with applications in

medicine, pesticides, cosmetics and is the raw material in many other chemical processes.<sup>4</sup> There are more than 70 compounds that can be synthesized from 5-MF.<sup>4</sup> Furthermore, due to its low oxygen content, high energy density and good solubility in hydrocarbons, 5-MF is also considered a better additive in gasoline than ethanol or a raw material for alternative fuels. For example, Corma et al. suggested a route for producing high quality diesel from 5-MF.<sup>5</sup> Unfortunately, the wide application of 5-MF has been strictly limited by the high cost of the current industrial synthesis route of 5-MF from 2-methylfuran and phosgene.<sup>4</sup>

Therefore, the synthesis of 5-MF from biomass-derived HMF has attracted increased attention, which requires the hydrogenolysis of a hydroxymethyl group while keeping aldehyde group unchanged.<sup>6</sup> As early as in 2014, Fu et al. reported 88% yield of 5-MF from hydrogenolysis of HMF with W<sub>2</sub>C/AC as catalyst under 4 MPa of H<sub>2</sub> in tetrahydrofuran (THF) solution.<sup>7</sup> Later, Hu et al. investigated the mechanism of preferential hydrogenation of hydroxymethyl group to aldehyde group in HMF over those W<sub>2</sub>C-based catalysts by computational method.<sup>8</sup> Kinetically, W-site enhances the hydro-dehydration of hydroxymethyl group and restrains the hydrogenation of aldehyde group due to its strong Lewis acidity. In 2017, Fu et al. reported the synthesis of DMF from HMF using Fe–N–C catalyst in butanol. As an intermediate, 5-MF can also be obtained at 22% yield.<sup>9</sup> Recently, Han and co-workers reported more than 99% yield of 5-MF under 4 MPa H<sub>2</sub> using Nb<sub>2</sub>O<sub>5</sub> supported single-atom Pt as catalyst.<sup>6,10</sup> In that study, Nb sites were reported to activate the C–OH

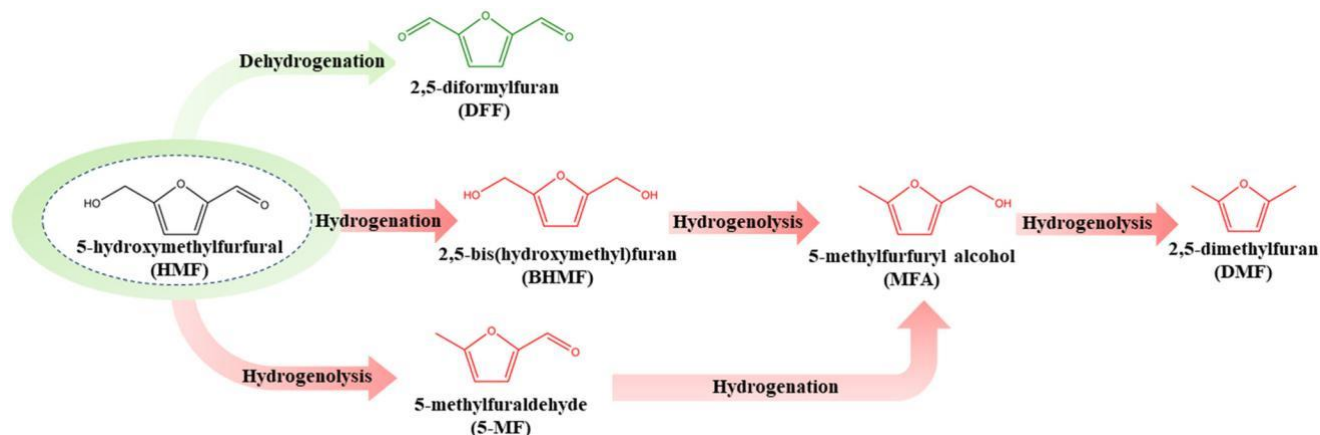
<sup>a</sup> Anhui Province Key Laboratory of Advanced Catalytic Materials and Reaction Engineering, School of Chemistry and Chemical Engineering, Hefei University of Technology, Hefei, Anhui, 230009, P.R. China. E-mail: yetq@hfut.edu.cn

<sup>b</sup> School of Materials Science and Engineering, Hefei University of Technology, Hefei, Anhui, 230009, P.R. China

<sup>c</sup> Research Institute of Petroleum Processing, Sinopec, Beijing, 100083, P.R. China

<sup>d</sup> Max Planck-Cardiff Centre on the Fundamentals of Heterogeneous Catalysis FUNCAT, Cardiff Catalysis Institute, School of Chemistry, Cardiff University, Cardiff CF10 3AT, UK. E-mail: carterj5@cf.ac.uk

† These authors contributed equally to this work.



Scheme 1 Chemicals derived from HMF under hydrogenation–dehydrogenation reaction conditions.

group, while Pt atom sites were considered responsible for the activation of hydrogen, and none of them can activate the C O group, hence the high selectivity of 5-MF obtained. In a similar way to Pt, Pd can also activate H<sub>2</sub> in this reaction. According to the density functional theory (DFT) study of the transformation of HMF on Pd(111), Cu(111) and Cu<sub>3</sub>Pd(111) surfaces,<sup>11</sup> the favorable dissociation of H<sub>2</sub> on Pd active sites makes the Cu<sub>3</sub>Pd a highly promising catalyst for the selective transforming HMF to DMF.

Besides H<sub>2</sub>, some other H-containing compounds could also act as the deoxidation agent.<sup>12</sup> Using Pd–PVP/C as catalyst and formic acid as hydrogen source, Sun et al. obtained 80% yield of 5-MF in THF solution.<sup>13</sup> Very recently, Bao et al. reported 95% yield of 5-MF in 1,4-dioxane using N-doped carbon layer-coated Au nanocatalyst and renewable formic acid (FA) as the deoxygenation reagent.<sup>14</sup> The above results indicate that hydrogenolysis of HMF to 5-MF could be done with the hydrogen produced in situ. In our previous work,<sup>15</sup> 7.8% yield of 5-MF was obtained as by-product from HMF dehydrogenation on Cu/Al<sub>2</sub>O<sub>3</sub> catalyst without H<sub>2</sub> addition, when use water as solvent. Although water not involved in the reaction equation as reactant of hydrogenolysis of HMF, it could enhance the reaction as a proton exchange medium. Moreover, for the reasons of environmental and health, it is more desirable to synthesis 5-MF from HMF in water.

We note that the oxidation of iron by water has been the subject of enormous interest for many years,<sup>16</sup> while we consider that insufficient attention has been paid to its catalytic application. In the present work, high productivity of 5-MF from HMF was realized using an Fe catalyst under atmospheric pressure in an aqueous solution and water acts as both solvent and reactant. The total reaction consists of two main steps, namely the reaction of Fe and H<sub>2</sub>O to produce hydrogen in situ and the subsequent hydrogenolysis of HMF. The catalytic performance and reaction mechanism were studied by the combination of experiments and DFT calculations.

## 2. Experimental

### 2.1 Materials

5-Hydroxymethylfurfural (HMF), 2,5-diformylfuran (DFF), 5-methylfuraldehyde (5-MF), ferric chloride hexahydrate, urea, acetonitrile, ethanol, iso-propanol, dimethyl sulfoxide (DMSO), 1,4-dioxane were purchased from Sinopharm Chemical Reagent Co., Ltd. All the chemicals were of analytical grade. The other chemicals including transition metal oxides were purchased from local companies and used without further purification. Ultrapure water was used for the catalyst preparation and catalytic reactions.

### 2.2 Catalyst preparation

The preparation method of Fe<sub>2</sub>O<sub>3</sub> catalyst is similar with that previously reported.<sup>17</sup> Firstly, a certain mass of urea was dissolved in 80 mL deionized water under magnetic stirring until a clear solution was formed. Then 4.32 g of ferric chloride hexahydrate was added into the urea solution. The obtained brown solution was stirred at room temperature for 10 min and in an ultrasonic bath for 20 min. The homogeneous solution was then loaded into high-pressure autoclaves and kept in an oven at 200 °C for 24 h. Then the precipitate was centrifuged and washed alternately with deionized water and ethanol until the pH of the wash solution equaled 7. The resulting product was dried overnight in an oven at 110 °C.

### 2.3 Catalyst characterization

Powder X-ray diffraction (XRD) was carried out using a PANalytical X'Pert Pro MPD with Cu K $\alpha$  radiation ( $\lambda = 0.154$  nm). The surface elements and their states were analyzed by X-ray photoelectron spectroscopy (XPS) implemented on an ESCALAB-250Xi (Thermo-VG Scientific, USA) spectrometer with Al K $\alpha$  (1486.6 eV) irradiation source. All binding energies (BEs) were corrected referencing the C1s (284.6 eV) peak of adventitious carbon as an internal standard. Temperature programmed reduction (TPR) of H<sub>2</sub> was

performed on a home-made apparatus under a 10 vol% H<sub>2</sub>/Ar gas flow (40 ml min<sup>-1</sup>) at a rate of 10 °C min<sup>-1</sup> up to 800 °C and using a thermal conductivity detector (TCD). Nitrogen adsorption experiments for pore size distribution, pore volume, and surface area measurements were conducted on a COULTER SA 3100 analyzer.

## 2.4 Catalytic reactions

The catalytic transformation of HMF was carried out in a home-made continuous flow fixed-bed reactor under atmospheric pressure. In a typical experiment, 0.2 g of the catalyst was placed into the quartz reactor. The catalyst bed was packed with silica wool which serves as the preheated zone, so the reactants can be vaporized here. Before reaction, catalysts were pre-reduced by a 50 vol% H<sub>2</sub>/N<sub>2</sub> stream at 500 °C for 2 h. The HMF dissolved in the solvent (typically 12.6 mg ml<sup>-1</sup>) was fed into the reactor (1 ml h<sup>-1</sup>) with a syringe pump. The reactions were conducted under H<sub>2</sub> (unless specified), keeping a constant flow rate of 20 ml min<sup>-1</sup> by using mass flow controllers.

The liquid product was condensed with an ice bath and analyzed offline by GC with an Agilent 7820A apparatus equipped with an HP-5 (30 m × 320 μm × 0.25 μm) capillary column and a flame ionization detector (FID). We calculated the HMF, DFF and 5-MF contents in the samples using an external standard calibration curve that had been constructed based on the pure compounds. Repeated runs showed that data variation was in the range of ±10% (relative value).

HMF conversion δ% ▽

$$\frac{1}{4} \frac{\text{Moles of HMF added} - \text{Moles of Unreacted HMF}}{\text{Moles of HMF added}} \times 100\%$$

5-MF Selectivity δ% ▽

$$\frac{1}{4} \frac{\text{Moles of 5-MF}}{\text{Moles of HMF added} - \text{Moles of unreacted HMF}} \times 100\%$$

The effluent containing deuterated products was collected in an ice-cold trap. These products were analyzed by an Agilent 7890A-5975C GC-MS system equipped with a HP-5MS (30.0 m × 250 μm, 0.25 μm). Before analyze, the products were extracted by CH<sub>2</sub>Cl<sub>2</sub>. <sup>1</sup>H NMR spectra was recorded at 25 °C by a 600 MHz VNMRs600 (Agilent Technologies Inc., USA) spectrometer using D<sub>2</sub>O as solvent.

## 2.5 Methods and models for DFT calculations

All calculations were performed using the Vienna ab initio simulation package (VASP).<sup>18</sup> The electron-ion interaction is described with the projector augmented wave (PAW) method. The generalized gradient approximation and the Perdew–Burke–Ernzerhof functional (GGA-PBE) were used to describe the exchange and correlation energies for all systems.<sup>19</sup> Spin polarization was considered for the magnetic properties of iron. The electronic wave functions were expanded in a plane

wave basis where the kinetic cut-off energy was 400 eV and the Gaussian electron smearing method with σ = 0.2 eV were used. The convergence criteria for the electronic self-consistent iteration and force were set to 10<sup>-6</sup> eV and 0.01 eV Å<sup>-1</sup>, respectively.

A 6 × 6 Fe(110) surface with a thickness of four atom layers was employed for all calculations. The bottom two layers was frozen, and the top two layers were allowed to relax. The vacuum layer between periodically repeated slabs was set as 15 Å to avoid interactions among slabs. The Brillouin zone was sampled with a 2 × 2 × 1 k-point grid. Surface relaxation was performed until all forces were smaller than 0.01 eV Å<sup>-1</sup>. Transition state structures and reaction barriers of elementary steps were located using the climbing image nudged elastic band (CI-NEB) or the dimer methods.<sup>20,21</sup> Vibrational analysis was performed at the same level of theory to verify the transition state with only one imaginary frequency.

The adsorption energies (E<sub>ad</sub>) are defined as

$$E_{ad} = E_{total} - (E_{surface} + E_{adsorbate}) \quad (1)$$

where E<sub>total</sub> is the total energy of the slab with adsorbed molecules in its equilibrium geometry; E<sub>surface</sub> is the total energy of the clean surface, and E<sub>adsorbate</sub> is the energy of the free adsorbate in the gas phase.

The activation energy was calculated as the difference in energy between the transition and initial state (IS), while the reaction energy (E<sub>r</sub>) was the energy difference between final state (FS) and initial state, according to the eqn (2) and (3) respectively.

$$E_a = E_{(TS)} - E_{(IS)} \quad (2)$$

$$E_r = E_{(FS)} - E_{(IS)} \quad (3)$$

## 3. Results and discussion

### 3.1 Catalytic performance in HMF hydrogenolysis

Although for these reactions, noble metal catalysts usually show better results than non-noble metals and are widely used in commercial, the search for non-noble alternatives has never stopped. Inspired by our previous work on Cu catalysts,<sup>15</sup> we further investigated other transition metals in the fourth period of the periodic table. HMF hydrogenolysis was typically carried out in a continuous flow fixed-bed reactor at 260 °C and ambient pressure. An aqueous solution of HMF (typically 12.6 mg mL<sup>-1</sup>) was used as the reactant and pumped into the reactor with a syringe. Liquid products were collected between 1.5 and 2 h.

As shown in Table S1,† the commercial Fe-based catalyst gives the highest HMF conversion of 84.2% and 5-MF selectivity of 75.8% respectively at 300 °C, much better than other commercial metal oxides. Therefore, we focused on iron-based catalysts to investigate the potential application in

HMF hydrogenolysis. Moreover, we compared the home-made iron-based catalyst with the commercial one. Although they showed similar 5-MF selectivity at 260 °C, the synthesized catalyst described in our study gives higher HMF conversion of 90.2%, which more than two times that achieved with a commercially sourced catalyst giving more than twice the yield of 5-MF. We attribute this difference to the higher surface area of the synthesized catalyst ( $12 \text{ m}^2 \text{ g}^{-1}$  versus  $7 \text{ m}^2 \text{ g}^{-1}$ ), thus more active centers and higher activity. Therefore, home-made Fe-based catalyst was mainly adopted in the following research works, unless otherwise specified.

The influence of atmosphere on catalytic performance of metal iron was then investigated. As Fig. 1 shows, most of the HMF polymerized to humins under oxidative atmosphere of air. 37.3% selectivity to DFF and only 1% selectivity to 5-MF were obtained, showing oxidative dehydrogenation is the dominant reaction path under these conditions besides polymerization. While under hydrogen, 5-MF was the only detectable product and the selectivity was 77.3%, indicating that HMF hydrogenolysis is facile.

Interestingly, 5-MF was also the main product even under inert atmosphere of nitrogen. The selectivity of hydrogenolysis product to 5-MF was 73.9%, very close to that under hydrogen atmosphere. Therefore, we speculate that HMF hydrogenolysis was mainly accomplished by hydrogen formed in situ from water decomposition on the iron surface, by the mechanism shown in Scheme 2.

To help demonstrate this, isotopic labeling experiments using deuterium oxide ( $\text{D}_2\text{O}$ ) were performed to understand the role of water in the hydrogenolysis of HMF. HMF was dissolved in  $\text{D}_2\text{O}$  and the catalytic reaction was repeated under  $\text{H}_2$  atmosphere as before. 5-MF was detected by mass spectrometry after separation from the reaction system. As can be observed from Fig. 2, the molecular ion peak shifted from the normal  $m/z = 110$  to 111, and the fragment ion  $m/z = 53$  shifted to 54. This indicates that hydrogen mainly comes from the water rather than gaseous  $\text{H}_2$ , during hydrogenolysis. Furthermore, dideuterium substituted products were also detected (at  $m/z = 112$  and  $m/z = 55$ ). To

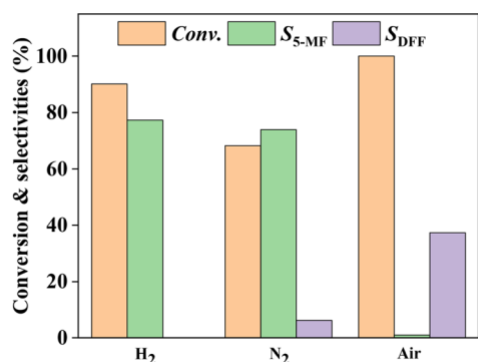
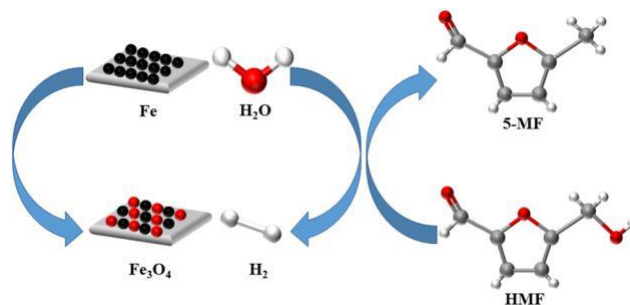


Fig. 1 Catalytic performance of Fe catalyst under various atmosphere at 260 °C.



Scheme 2 Mechanism of hydrogenolysis of HMF with  $\text{H}_2\text{O}$  on iron surface.

investigate the position of the second deuterium, the product was further analyzed by  $^1\text{H}$  NMR. As shown in the Fig. S1,† the  $^1\text{H}$  NMR spectrum of the 5-MF in  $\text{D}_2\text{O}$  had four resonances: two from the furan ring and one from the formyl

–CHO proton signals at 6.37, 7.44 and 9.26 ppm respectively. These three signals gave similar relative integrated intensities, consistent with the molar ratio of 1 : 1 : 1 in 5-MF. The signal at 2.37 ppm represents three protons from the methyl group. However, in deuterated 5-MF product as shown in Fig. S2,† this signal moved to around 2.35 ppm and the integrated intensity is only 1.45 times of the other signals, showing the second deuterium is also on the methyl group which may substitute by H–D exchange.

The reaction rate is higher in  $\text{H}_2\text{O}$  than in  $\text{D}_2\text{O}$ . As shown in Fig. S3,† the HMF conversion decreased from 47.2% in  $\text{H}_2\text{O}$  to 42.3% in  $\text{D}_2\text{O}$ , while the 5-MF selectivity increased from 65.9 to 73.5%. This kinetic isotope effect confirms that water directly participates in the reaction.

We noticed that in almost all previous reports of 5-HMF hydrogenolysis to 5-MF, organic compounds were used as solvents, which is not desirable from a green chemistry perspective. Table S2† shows a summary of literature reports, which have been mainly carried out in the liquid phase. The key differences between the current work and the literature reports are that the gas-phase transformation takes place at higher temperature ( $>260$  °C) than the liquid phase reaction ( $>140$  °C), which also requires relatively high pressures of  $\text{H}_2$  (typically  $>10$  bar) or other H donor (isopropyl alcohol or formic acid). In the current work, it has been shown that

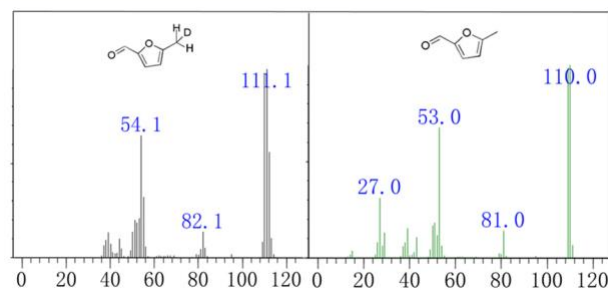


Fig. 2 React with  $\text{D}_2\text{O}$  and  $\text{H}_2\text{O}$  respectively under  $\text{H}_2$  atmosphere at 260 °C.

H<sub>2</sub>O can in principle be used in place of high pressures of H<sub>2</sub>. The space time yield (STY) of the literature reports has also been calculated and is in the range of 0.12–5.98 mmol 5-MF g<sub>cat</sub><sup>-1</sup> h<sup>-1</sup>. The STY of the Fe catalyst prepared in the current work was 0.73 mmol 5-MF g<sub>cat</sub><sup>-1</sup> h<sup>-1</sup> when in mixture solvent.

According to the numerous previous reported works in autoclave reactor, the solvent plays an important role in the hydrogenolysis of HMF. In fact, most of them were performed in various organic solvents to obtain better conversion or selectivity. Therefore, to investigate the influence of solvent on the metallic Fe catalyst in continuous flow fixed-bed reactor, we also tested some of the organic solvents. As shown in Table 1, 40.8% selectivity of 5-MF was obtained when using isopropyl alcohol as solvent which is unsurprising as it is used as hydrogen donor in some reactions.<sup>22</sup> On the contrary, almost all of the HMF polymerized to undetectable product when using acetonitrile and 1,4-dioxane as solvents.

The effect of 1,4-dioxane as a co-solvent with water was also investigated. The HMF concentration was raised to 25.2 mg ml<sup>-1</sup> in this experiment to keep conversions under 100%. As shown in Fig. 3, the HMF conversion increased gradually from 47.2% in pure water to 85.8% with 75 wt% 1,4-dioxane. The 5-MF selectivity was also the highest at 75 wt% 1,4-dioxane, where it was measured to be 84.9%. This may be ascribed to the better dispersion and easier gasification of HMF in the mixed solvent. This effect was also observed by Yu et al. in the catalytic reaction of furfural oxidation.<sup>23</sup> 1,4-Dioxane without water gave 100% conversion of HMF and extremely low 5-MF selectivity (8%), as expected.

Iron could exist in many valence states and phases under the adopted reaction conditions, such as Fe, Fe<sub>3</sub>O<sub>4</sub>, Fe<sub>2</sub>O<sub>3</sub>, and/or their mixture. Therefore, the influence of reduction temperature on the catalytic performance was studied to obtain an optimized catalyst composition. Catalysts reduced at 400, 500, 600 °C, together with an unreduced sample were prepared. Catalytic reactions were carried out at 260 and 300 °C and the results are shown in Table 2. The catalyst reduced at 500 °C showed high yield of 5-MF both at 260 and 300 °C, while the unreduced sample gave much higher selectivity to dehydrogenation product of DFF. The 400 °C reduced sample showed 72.2% selectivity to 5-MF and 8.4% selectivity to DFF at 260 °C and at 300 °C this increased to 29.8%. The 600 °C reduced sample showed low conversion and selectivity to 5-MF compared with the other reduced samples.

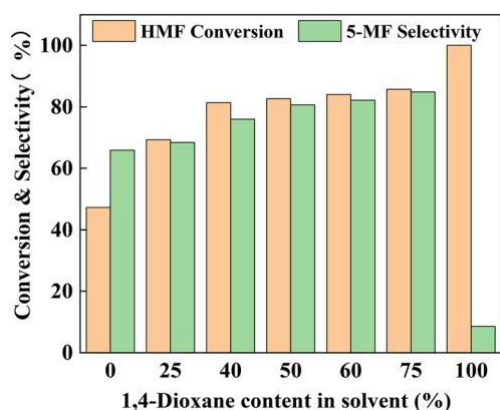


Fig. 3 The influence of 1,4-dioxane contents in water on the catalytic performance (reaction condition: 25.2 mg ml<sup>-1</sup> of HMF in mixture solvents, 1 ml h<sup>-1</sup> feed speed, 300 °C).

### 3.2 Characterization of catalysts

To understand the different catalytic performance under various conditions, XRD analysis was firstly carried out to identify the phase of fresh, reduced and used catalysts. As can be seen from Fig. 4(A), the fresh catalyst showed characterization peaks at 2θ = 33.2, 35.6, 54.1° which is the typical Fe<sub>2</sub>O<sub>3</sub> diffraction pattern (PDF No. 33-0664).<sup>24</sup> After reduction by hydrogen at 500 °C, the diffraction peaks of Fe<sub>2</sub>O<sub>3</sub> disappeared, while characteristic diffraction peaks of metallic iron (PDF No. 06-0696) emerged at 44.6 and 65.0°, due to the crystal faces (110) and (200), respectively. The chemical states of the surface Fe species were investigated by XPS analysis (Fig. S4†). The peak centered at 705.7 eV could be attributed to metallic iron, showing the reduction of iron oxide,<sup>25</sup> which is consistent with the XRD results. However, deconvolution of the XPS profile revealed BE values of 709.6 and 710.8 eV (29% and 55% content respectively), which were ascribed to Fe<sup>2+</sup> and Fe<sup>3+</sup> species respectively. The surface iron oxide was ascribed to the contact with air during sample preparation.

Revealed by the XRD pattern shown in Fig. 4(A), the Fe catalyst re-oxidized to Fe<sub>3</sub>O<sub>4</sub> (PDF No. 26-1136) after use in hydrogenolysis of HMF at 260 °C for 24 h. The characteristic reflections of Fe<sub>3</sub>O<sub>4</sub> at 2θ = 30.1, 35.4, 57.0 and 62.6° were observed, while the reflections of metallic iron disappeared. To evaluate the degree of re-oxidation, TPR measurements of fresh and used catalysts were carried out and reported in Fig. 5. The pristine Fe<sub>2</sub>O<sub>3</sub> sample showed two distinctive

Table 1 Catalytic performance in various solvents at 300 °C

Solvents	C (%)	S <sub>5-MF</sub> (%)	S <sub>DFF</sub> (%)	S <sub>hum</sub> (%)	Y <sub>5-MF</sub> (%)
Water	100.0	69.0	0	31.0	69.0
Isopropyl alcohol	79.3	40.8	0	59.2	32.4
Acetonitrile	93.2	1.1	0	98.9	1.0
1,4-Dioxane	100.0	0.6	0	99.4	0.6
DMSO <sup>a</sup>	43.2	0	0	100.0	0.0

<sup>a</sup> DMSO: dimethyl sulfoxide.

Table 2 Catalytic performance of Fe catalyst with various reduction temperature

Reduction temperature (°C)	260 °C				300 °C			
	C (%)	S <sub>5</sub> -MF (%)	S <sub>DFF</sub> (%)	Y <sub>5</sub> -MF (%)	C (%)	S <sub>5</sub> -MF (%)	S <sub>DFF</sub> (%)	Y <sub>5</sub> -MF (%)
Unreduced	97.4	21.4	26.2	20.8	87.5	40.8	40.8	35.7
400	97.6	72.2	8.4	70.5	98.2	48.4	29.8	47.5
500	90.5	77.3	0.0	70.0	100.0	69.0	0.0	69.0
600	21.5	55.2	10.9	11.9	37.7	43.4	7.0	16.4

reduction peaks centered at 353 and 549 °C, which were attributed to the reduction of Fe<sub>2</sub>O<sub>3</sub> to Fe<sub>3</sub>O<sub>4</sub> and Fe<sub>3</sub>O<sub>4</sub> to Fe respectively. For the used sample, only the reduction peak of Fe<sub>3</sub>O<sub>4</sub> to Fe could be observed, due to Fe<sub>3</sub>O<sub>4</sub> being the main phase. Calculated from the peak area of TPR profile, the elemental composition of used sample can be expressed as FeO<sub>0.34</sub>, indicating only partial re-oxidation occurred. Since the oxygen amount from HMF is too small to generate that degree of re-oxidation, we speculate the re-oxidation was mainly done by water. To further confirm it, the reduced catalyst was exposed to water vapor carried by nitrogen under normal reaction temperature of 260 °C for 4 h. After that, TPR analysis was performed. A similar profile with the used sample was obtained, as can be seen from Fig. 5(c). The vapor treated sample can be expressed as FeO<sub>0.25</sub> according to the calculated peak area of TPR profile.

The catalysts reduced at various temperatures were examined by XRD after 4 h reactions. According to the previous discussion, the catalyst reduced at 500 °C showed typical XRD pattern of metallic iron, indicating thorough reduction. However, after 4 h reaction, Fe<sub>3</sub>O<sub>4</sub> phase emerged due to the re-oxidation by water, as shown in Fig. 4(B). In the 600 °C reduced sample, no diffraction peaks of Fe<sub>3</sub>O<sub>4</sub> were observed and the catalyst still maintained the metallic iron phase, which indicates that the 600 °C reduced sample was could not re-oxidize under the reaction conditions, this may be the reason of low HMF conversion. In contrast, the 400 °C reduced sample mainly re-oxidized to Fe<sub>3</sub>O<sub>4</sub>. These results once again prove that hydrogenolysis of HMF is induced by H<sub>2</sub> in situ

produced from water dissociation on the metallic iron surface, while high valence Fe<sup>2+</sup>/Fe<sup>3+</sup> is more conducive to dehydrogenation reaction route.

It was considered that re-oxidation could decrease 5-MF selectivity and catalyst activity, therefore stability and reusability tests were performed at 280 °C. The catalyst was subjected to five testing cycles, and each run lasted for 8 h. After each run, catalyst was reduced in 50 vol% H<sub>2</sub>/Ar for 2 h at 500 °C for regeneration. The results are summarized in Fig. 6. In each run, both HMF conversion and 5-MF selectivity decreased slowly on-stream, which was due to the accumulation of surface oxygen according to discussion above. Although the regeneration process could recover the catalyst entirely, the HMF conversion and 5-MF selectivity decreased slightly between the cycles. The observed highest conversion in cycle 1 was 100%, which decreased to 95.2% in cycle 5. And the highest selectivity in cycle 1 is 75.8%, which decreased to 67.7% in cycle 5. The results indicate the metallic iron catalyst still needs further improvement to meet the needs of industrialization, which is our topic of interest in the near future.

### 3.3 Computational studies

To better understand the microscopic reaction mechanism of HMF hydrogenolysis with water on iron metal surface, DFT was employed to calculate the energy changes of some steps of the adsorption and reaction route. According to Liu et al., dispersion corrections always overestimate the dispersion interactions of not only the weakly adsorbed H<sub>2</sub>O molecule

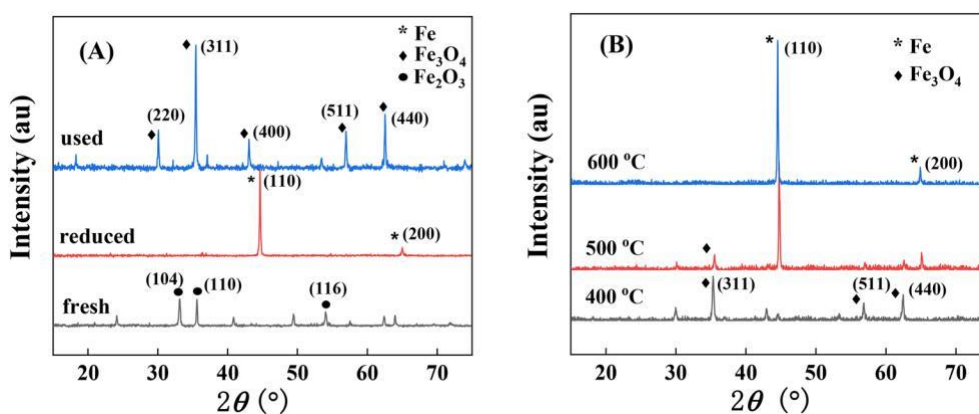


Fig. 4 XRD patterns of the Fe catalysts (A: fresh, reduced at 500 °C for 2 h and used at 260 °C for 24 h; B: used catalysts which reduced at various temperatures).

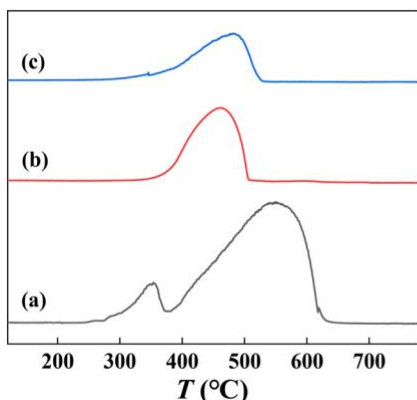


Fig. 5 TPR profiles of (a) fresh catalyst, (b) after used at 260 °C for 4 h and (c) exposed to vapor at 260 °C for 4 h.

but also the strongly adsorbed  $H_2$  molecule on the low-index surface of Fe(100). Therefore, dispersion interactions were not adopted in this work.<sup>16</sup> The calculated adsorption energy of water on Fe(110) surface is  $-0.36$  eV, very similar to reported  $-0.41$  eV on Fe(100).

As shown in Fig. 7, four plausible adsorption configurations of HMF on Fe(110) surface were considered:

(a) flat configuration in which the furan ring parallel to the surface, (b) tilted configuration in which the furan ring tilted away, (c) upright adsorption of the carbonyl group and (d) upright adsorption of the hydroxyl group. The calculated adsorption energies are  $-2.05$ ,  $-0.76$ ,  $-0.63$  and  $-0.32$  eV respectively. Therefore, flat configuration is the most favoured in terms of energy. However, the ultrahigh adsorption energy indicated a super strong affinity of HMF toward the Fe(110) surface, which is no good for the subsequent reactions. Similar with Pt, Pd and Ni, the super strong interaction between metal iron and furan ring may originating from a  $sp^2$ -to- $sp^3$  rehybridization.<sup>2</sup> We further compared the adsorbate arrangements of 5-MF product on Fe(110) surface with flat and tilted configuration. The adsorption energies were  $-1.70$  and  $-0.80$  eV respectively. The

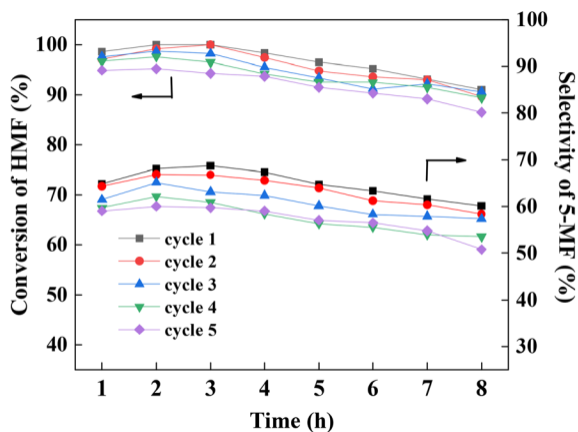


Fig. 6 Time-on-stream data for metal iron catalyst in HMF hydrogenolysis.

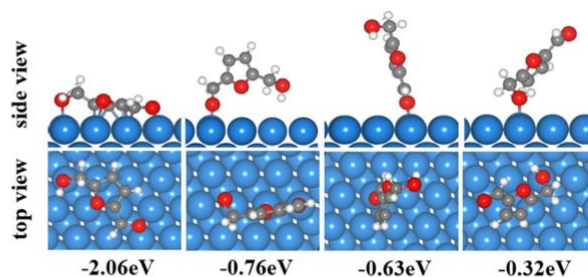


Fig. 7 Adsorption configurations of HMF over Fe(110) surface.

ultrahigh desorption energy of 5-MF product is another disadvantage of flat configuration. That may be the reason of high selectivity to humins on the Fe catalyst. According to the above results, the tilted adsorption configuration of HMF was chosen for the next studies.

The important role of  $H_2O$  in the hydrogenolysis of HMF has been proved by the experimental results as discussed above. Therefore, the reaction pathway of HMF together with water on Fe(110) was calculated by DFT. A plausible reaction route was identified and shown in Fig. 9. The reaction begins with the co-adsorption of HMF and  $H_2O$ . The second step is the dissociation of adsorbed  $H_2O$ . Similar with the reported results on Fe(100),<sup>16</sup> it's also facile to perform on Fe(110) with a barrier of 0.251 eV. The third step is the exchange of hydrogen from the dissociation of  $H_2O$  and the hydroxyl group from HMF to form the product 5-MF: the barrier is 0.425 eV. From the above results, we can see that the energy barriers for those steps are relatively low. In fact, the most energy demanding step is the desorption of product 5-MF from Fe(110) surface as Fig. 8 shows.

Moreover, after hydrogenolysis, the two OH species left on the surface could disproportionate to form molecular  $H_2O$  and surface O atom. Therefore, the total result is HMF gives an O atom to Fe catalyst and water acts as a hydrogen donor. As the reaction proceeds, the metallic iron catalyst will be re-oxidized to iron oxide and need reduction process.

To sum up, water induced hydrogenolysis of HMF has low energy barriers in the investigated reaction coordinate. This may be the reason of the high 5-MF selectivity on Fe catalyst

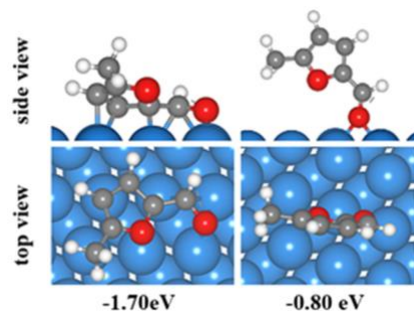


Fig. 8 Adsorption configurations of 5-MF over Fe(110) surface.

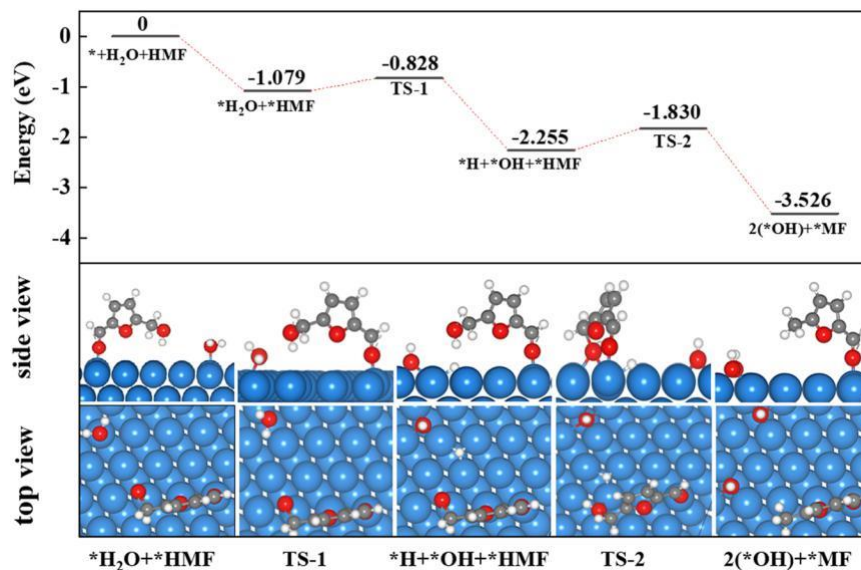


Fig. 9 Reaction coordination of HMF hydrogenolysis on Fe(110) surface.

with water as solvent. However, the unsatisfactory carbon balance may be attributed to the high desorption energy of 5-MF and strong affinity of HMF toward the iron surface in a flat configuration.

## 4. Conclusions

In summary, iron catalyzed hydrogenolysis of HMF was performed at ambient pressure on continuous flow fixed-bed reactor. Both catalyst preparation and reduction temperature have an impact on catalytic performance. Water is not only the optimized solvent, but crucially, also acts as the hydrogen donor. Therefore, even under inert atmosphere of  $N_2$ , the hydrogenolysis of HMF can be carried out with fairly high productivity.  $^1H$  NMR and GC-MS analysis of the deuterated product confirmed that the hydrogen was mainly come from water instead of gaseous  $H_2$ , although catalytic performance under  $H_2$  atmosphere is slightly improved than under inert atmosphere. That said, from a process point of view, it is desirable to avoid flammable reagents such as gaseous  $H_2$ . DFT calculations were adopted to help understand the mechanisms of water induced HMF hydrogenolysis on metallic iron catalyst. The high 5-MF selectivity on Fe catalyst may be attributed to the low energy barriers in the investigated reaction coordinate, while the unsatisfactory carbon balance mainly attributed to the high desorption energy of 5-MF product.

The humin formation may be explained by the polymerization of the furanic compounds on the Lewis acidic sites of the catalyst. However, it can be improved to some extent by optimizing reaction conditions. Though, compared with those catalyzed by noble metal catalysts in organic solvent, this catalytic system needs better understanding and further improvement to meet the needs of industrialization, which will be the subject of our future work.

## Conflicts of interest

The authors declare that they have no known competing financial interests or personal relationships that could have appeared to influence the work reported in this paper.

## Acknowledgements

The project was supported by Hefei Municipal Natural Science Foundation (2021043) and the Fundamental Research Funds for the Central Universities (JZ2017HG TB0231).

## References

- 1 R. Gerardy, D. P. Debecker, J. Estager, P. Luis and J. M. Monbaliu, *Chem. Rev.*, 2020, 120, 7219.
- 2 S. Chen, R. Wojcieszak, F. Dumeignil, E. Marceau and S. Royer, *Chem. Rev.*, 2018, 118, 11023.
- 3 H. Xia, S. Xu, H. Hu, J. An and C. Li, *RSC Adv.*, 2018, 8, 30875.
- 4 Y. Peng, X. H. Li, T. Gao, T. Li and W. R. Yang, *Green Chem.*, 2019, 21, 4169.
- 5 G. W. Huber, S. Iborra and A. Corma, *Chem. Rev.*, 2006, 106, 4044.
- 6 S. P. Li, M. H. Dong, J. J. Yang, X. M. Cheng, X. J. Shen, S. L. Liu, Z. Q. Wang, X. Q. Gong, H. Z. Liu and B. X. Han, *Nat. Commun.*, 2021, 12, 584.
- 7 Y. B. Huang, M. Y. Chen, L. Yan, Q. X. Guo and Y. Fu, *ChemSusChem*, 2014, 7, 1068.
- 8 W. Tai, S. Fu, T. H. Liu, H. Q. Yang and C. W. Hu, *ChemSusChem*, 2022, 15, e202200174.
- 9 J. Li, J. J. Zhang, H. Y. Liu, J. L. Liu, G. Y. Xu, J. X. Liu, H. Sun and Y. Fu, *ChemistrySelect*, 2017, 2, 11062.
- 10 S. Li, J. Du, B. Zhang, Y. Liu, Q. Mei, Q. Meng, M. Dong, J. Du, Z. Zhao, L. Zheng, B. Han, M. Zhao and H. Liu, *Acta Phys.-Chim. Sin.*, 2022, 38, 2206019.

- 11 R. Gunawan, H. S. Cahyadi, R. Insyani, S. K. Kwak and J. Kim, *J. Phys. Chem. C*, 2021, **125**, 10295.
- 12 L. Hu, N. Li, X. L. Dai, Y. Q. Guo, Y. T. Jiang, A. Y. He and J. X. Xu, *J. Energy Chem.*, 2019, **37**, 82.
- 13 G. H. Sun, J. H. An, H. Hu, C. Z. Li, S. L. Zuo and H. A. Xia, *Catal. Sci. Technol.*, 2019, **9**, 1238.
- 14 J. Zhang, Z. J. Wang, M. G. Chen, Y. F. Zhu, Y. M. Liu, H. Y. He, Y. Cao and X. H. Bao, *Chin. J. Catal.*, 2022, **43**, 2212.
- 15 B. Chen, X. Li, P. Rui, Y. Ye, T. Ye, R. Zhou, D. Li, J. H. Carter and G. J. Hutchings, *Catal. Sci. Technol.*, 2022, **12**, 3016.
- 16 S. Liu, X. Tian, T. Wang, X. Wen, Y.-W. Li, J. Wang and H. Jiao, *J. Phys. Chem. C*, 2014, **118**, 26139.
- 17 M. Su, C. He and K. Shih, *Ceram. Int.*, 2016, **42**, 14793.
- 18 G. Kresse and J. Furthmüller, *Phys. Rev. B: Condens. Matter Mater. Phys.*, 1996, **54**, 11169.
- 19 J. Perdew, K. Burke and M. Ernzerhof, *Phys. Rev. Lett.*, 1996, **77**, 3865.
- 20 G. Henkelman and H. Jónsson, *J. Chem. Phys.*, 1999, **111**, 7010.
- 21 G. Henkelman, B. P. Uberuaga and H. Jónsson, *J. Chem. Phys.*, 2000, **113**, 9901.
- 22 J. He, L. Schill, S. Yang and A. Riisager, *ACS Sustainable Chem. Eng.*, 2018, **6**, 17220.
- 23 X. Yu, M. Zuo, W. Jia, J. Chen, Y. Sun, X. Tang, X. Zeng, S. Yang, Z. Li, Z.-J. Wei, F. Xu and L. Lin, *Biomass Bioenergy*, 2022, **167**, 106642.
- 24 S. Elbasuney and M. Yehia, *J. Inorg. Organomet. Polym. Mater.*, 2019, **30**, 706.
- 25 P. C. J. Graat and M. A. J. Somers, *Appl. Surf. Sci.*, 1996, **100**, 36.